Research Article | Vol. 27, No. 5 | 4 Mar 2019 | OPTICS EXPRESS 6734
Optics EXPRESS

Efficient nitrogen-vacancy centers' fluorescence excitation and collection from micrometer-sized diamond by a tapered optical fiber in endoscope-type configuration

D. DUAN,[1,*] G. X. DU,[1,2] V. K. KAVATAMANE,[1] S. ARUMUGAM,[1] Y.-K. TZENG,[3,4] H-C CHANG,[3] AND G.BALASUBRAMANIAN,[1,5,6]

[1]*Max-Planck Research Group Nanoscale Spin Imaging, Max Planck Institute for Biophysical Chemistry,Am Fassberg 11,Göttingen, 37077, Germany*
[2]*Current address:School of Telecommunication and Information Engineering,Nanjing University of Posts and Telecommunications, Nanjing,China*
[3]*Institute of Atomic and Molecular Sciences, Academia Sinica, Taipei 106, Taiwan*
[4] *Stanford University, Stanford, California 94305, USA*
[5]*Center for Nanoscale Microscopy and Molecular Physiology of the Brain (CNMPB), Göttingen, 37077, Germany*
[6]*gbalasu@gwdg.de*
[*]*dduan@gwdg.de*

Abstract: Using an optical fiber to both excite the nitrogen-vacancy (NV) center in diamond and collect its fluorescence is essential to build NV-based endoscope-type sensor. Such endoscope-type sensor can reach inaccessible fields for traditional NV-based sensors built by bulky optical components and extend the application areas. Since single NV's fluorescence is weak and can easily be buried in fluorescence from optical fiber core's oxide defects excited by the green laser, fixing a micrometer size diamond containing high-density NVs rather than a nanodiamond containing single NV or several NVs on the apex of an optical fiber to build an endoscope-type sensor is more implementable. Unfortunately, due to small numerical aperture (NA), most of the optical fibers have a low fluorescence collection efficiency, which limits the sensitivity and spatial resolution of the NV-based endoscope-type sensor. Here, using a tapered optical fiber (TOF) tip, we significantly improve the efficiency of the laser excitation and fluorescence collection of the NV ensembles in diamond. This could potentially enhance the sensitivity and spatial resolution of the NV-based endoscope-type sensor. Numerical calculations show that the TOF tip delivers a high NA and has a high NV excitation and fluorescence collection efficiency. Experiments demonstrate that such TOF tip can obtain up to over 7-fold excitation efficiency and over 15-fold fluorescence collection efficiency of that from a flat-ended fiber (non-TOF) tip.

1. Introduction

In a classic experiment of using the negatively charged Nitrogen-vacancy (NV) color center in diamond as a sensor, the spin state of the NV center is initialized and detected by light guided through optical components such as objectives, lenses, and dichroic mirrors [1–7]. The bulky size and poor flexibility of these optical components limit its portability and flexibility. Using an optical fiber to replace these bulk components and built an NV-based endoscope-type sensor will greatly extend its potential application areas.

In the past years, some research groups have integrated NV-containing diamond in an optical fiber to explore its potential application areas. They are mainly in three categories: I. directly embedding nanodiamond inside an optical fiber or on an optical fiber end-face [8–12], II. using a tapered single mode optical fiber to couple the fluorescence from single NV center in nanodiamond

#351237 https://doi.org/10.1364/OE.27.006734
Journal © 2019 Received 8 Nov 2018; revised 24 Dec 2018; accepted 27 Dec 2018; published 22 Feb 2019

Optics EXPRESS

or diamond nanostructures [13–20], and III. directly position a micrometer size diamond on a multimode optical fiber [21–24]. Both I and II used diamond containing a single NV center or a few NV centers. Though some have reached a very high fluorescence collection efficiency, (E.g. using tapered single-mode fiber to collection fluorescence from diamond nanostructure [20],) they still rely on an objective lens to focus the green laser to the NV center, because single NV's fluorescence is weak and can easily be buried in fluorescence from optical fiber core's oxide defects excited by the green laser. Thus, they are not implementable for building an NV-based endoscope-type sensor. III, used a multimode optical fiber to both excite and read NV centers in a micrometer size diamond, is an endoscope-type sensor configuration. However, most of the multimode optical fibers have a small numerical aperture (NA) which limited its fluorescence collection efficiency. Since the NV's collected fluorescence of each measurement is directly linked to its minimum detectable variation [1, 2], the small fluorescence collection efficiency will limit the sensitivity and spatial resolution of the NV-based endoscope-type sensor. The specially designed high NA photonic microstructure optical fiber/ photonic crystal fibers can solve this problem [24]. However, the design and fabrication of such optical fiber is expensive and time-consuming.

Here, we demonstrate a method that efficiently excites NV centers in micrometer-sized diamond crystal and collects its emission fluorescence through the same optical fiber. We use a quasi-adiabatic tapered optical fiber (TOF) tip made from a multimode optical fiber (c.f. Fig. 1(a)) to concentrate the excitation laser on to the diamond, and at the same time, to collect the fluorescence from the diamond with a high efficiency. The TOF tip is equivalent to a high NA objective on the optical fiber. Numerical calculations show that such TOF tip delivers an ultra-high NA larger than 1.0 and has a high fluorescence excitation and collection efficiency. Experiments demonstrate that when exciting and collecting fluorescence from a ~5-μm diamond, such TOF tip can achieve over 7-fold the fluorescence excitation efficiency and over 15-fold the fluorescence collection efficiency of that from a flat-ended fiber (non-TOF) tip (Table 1). Optically Detected Magnetic Resonance (ODMR) scanning experiments demonstrated that this TOF tip could boost the DC magnetic field sensitivity of a micro-sized NV-based endoscope-type sensor. In a simple DC magnetic field measuring, a TOF based ~7.9-μm diamond NV-magnetometer achieve 1/28 the sensitivity value of a non-TOF tip based ~11.4-μm diamond NV-magnetometer, reaching a sensitivity of 180nT/$\sqrt{Hz}$. A practical use of such kind of TOF tip based endoscope-type configuration in measuring RF B-field of a small helical antenna is carried out by one author of us in literature [25].

2. Principles and methods

The TOF concept stems from the adiabatic taper of single-mode fiber. Decreasing the diameter shrinking rate along the optical fiber reduces its light transmission loss. When the shrinking rate is smaller than a certain value, the transmission loss can almost be ignored [26, 27]. Through multiple total internal reflections, the slowly shrinking TOF condenses the 532-nm laser from the multimode fiber core into the thin TOF tip, and at the same time, guides the fluorescence that entered the TOF tip within its maximum acceptance angle into the core of multimode fiber (Fig. 1(a) and Fig. 2(a)). This nearly adiabatic process enhances the NV centers excitation and fluorescence collection efficiencies. Calculation (using geometric ray optics) shows that the TOF tip's fluorescence collection efficiency can reach ~16 times that of a non-TOF tip (Fig. 2(b) and 2(c)) (when taking $n_{di} \approx 2.4$ as the diamond's refractive index). Experiments demonstrated that a long TOF (tip diameter: ~ 7.4 μm, length: ~ 15 mm) has collected 15.03 times the fluorescence of a non-TOF tip from the same 5μm diamond (Table 1). Simulation examples of multiple reflections from both fluorescence collection and NV excitation between TOF tip and non-TOF tip are shown in Fig. 3.

Optics EXPRESS

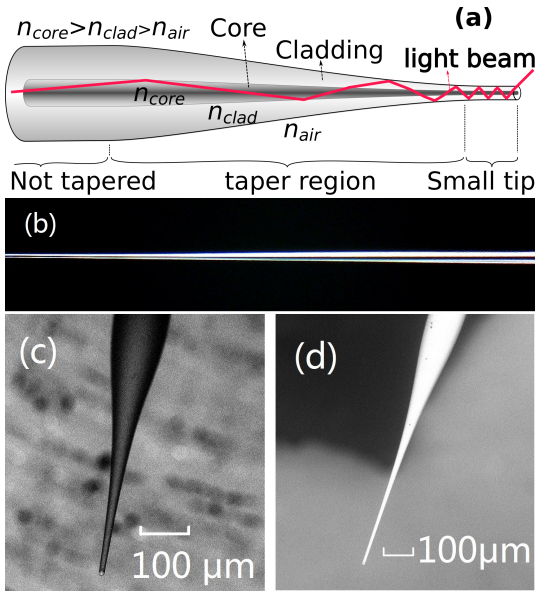

Fig. 1. The tapered optical fiber (TOF) tip. (a) Schematic diagram of the light ray trace that resulting in the high NA for the multimode optical fiber based TOF tip. (b) Optical microscope image of part of a long TOF tip's tapered region (total TOF length is ~15 mm, the photo is taken with 50 times magnification). Scanning electron microscope (c) side view and (d) 45-degree view of a short TOF tip with a length of ~1 mm.

2.1. Preparing of TOF tip and diamonds

The optical fiber we used is a graded index multimode fiber (GIF625, Thorlabs. Core diameter: 62.5 μm, cladding diameter:125 μm, NA : 0.275±0.015 at 850 nm, fiber core dopants: germanium whose fluorescence is not in the wavelength range of NV). The TOF tip was fabricated by first stretching the optical fiber under heating and then cutting the taper at its waist. By adjusting the heating and stretching force, the taper profile (shape) can be modified. More details about available tapering techniques to control the taper profile and its optical property have been previously reported in the literature [29–33]. We fabricated two kinds of TOF tips: one, long TOF tip tapered under flame heating with a slow diameter shrinking rate along the TOF (Fig. 1(b), with length longer than ~ 10 mm), and two, short TOF tip tapered under arc charging heating of an optical fusion splicer with a fast diameter shrinking rate along the TOF (Fig. 1 (c) and 1(d), with length shorter than ~1.5 mm).

The diamonds were prepared by irradiating the high-temperature high-pressure (HPHT) synthetic monocrystalline diamond powders with 3-MeV H+ to form the vacancies in the diamond. Subsequently the diamond samples were annealed in vacuum at 800 ^{o}C for approximately two hours to concentrate the nitrogen and vacancies [34]. The diamond powder we studied is industry grade; its shape is irregular, but the surface is flat and smooth.

2.2. TOF tip collection efficiency calculation

An acceptance angle θ_{max} related solid angle divided by 4π is its collection efficiency (Fig. 2(a)). Taking the diamond attached on the fiber tip surface as a thin sheet point sources ensemble, the fiber tip's collection efficiency is

$$\eta = \frac{2\pi[1 - cos(\theta_{max})]}{4\pi} = \frac{1 - cos(\theta_{max})}{2} \quad (1)$$

Optics EXPRESS

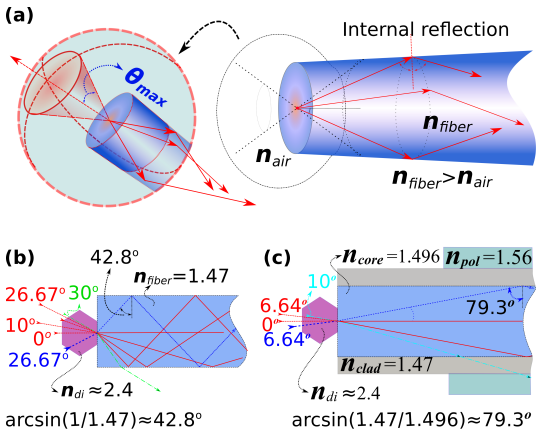

Fig. 2. Schematic of the collection efficiency calculation in case of TOF tip and flat-ended fiber (non-TOF) tip. (a) is the fiber light collection 3D illustration (solid angle). (b) and (c) are fluorescence acceptance angles of the TOF tip and non-TOF tip respectively when collecting light from an attached diamond.

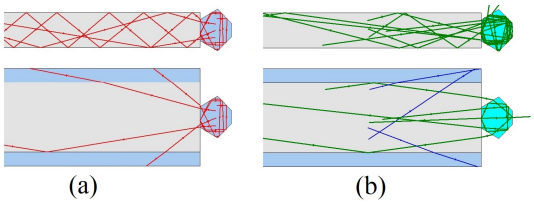

Fig. 3. Simulation of multiple reflections in (a) NV fluorescence collection and in (b) NV excitation for both TOF tip (top) and non-TOF tip (bottom). In (a), the original fluorescence rays are directed in 2°, 171°, 203° and 186° from same points/positions of the diamond in both the diamonds respectively. At the bottom of (b), the rays (blue) do not enter the diamond and do not exist, as un-tapered optical fiber does not support rays in such big angles. They are drawn for comparison. (The simulation is carried out by free software Optgeo [28])

NA is defined as $NA = \sqrt{n_{core}^2 - n_{clad}^2} = 0.275$ for the used optical fiber; n_{core} is the refractive index of the fiber core and n_{clad} is the refractive index of the fiber cladding. Taking the group refractive index of GIF625 fiber (1.496 at 850 nm) as the n_{core}; then the cladding refractive index of the fiber $n_{clad} \approx 1.47$. Ignoring the refractive index distribution in the cross-section of the TOF tip and treating it as the core with air surrounding it as the cladding. The maximum acceptance angle of the TOF tip is calculated according to Fig. 2(b).

$$\theta_{max} = arcsin[\frac{sin(\pi/2 - arcsin(n_{clad}/n_{core})}{n_{di}} \times n_{core}] \tag{2}$$

Taking $n_{di} \approx 2.4$ as the refractive index of diamond, $n_{fiber} = n_{clad} \approx 1.47$ as the TOF tip's refractive index and $n_{clad} = n_{air} \approx 1$, a maximum acceptance angle of $\theta_{max} = 26.7°$ is obtained for the TOF tip (Fig. 2(b). Taking $n_{fiber} = n_{core} \approx 1.496$ as the TOF tip's refractive index will rise θ_{max} a bit higher to 27.6°). Using equation (1), the TOF's collection efficiency can reach $\eta_d \approx 5.3\%$ in collecting fluorescence from an attached diamond. For the non-TOF tip, taking $n_{core} = 1.496$ and $n_{clad} = 1.47$, using equation (2) we obtained $\theta_{max} \approx 6.6°$ and the collection efficiency $\eta_{0.275d} \approx 0.32\%$ for accepting fluorescence from a contacted diamond (Fig. 2(c)). The TOF tip's fluorescence collection efficiency is ~ 16 times of a non-TOF tip. Taking

Optics EXPRESS

$\theta_{max} = 26.7°$ the calculated NA = $n_{di} \times sin(\theta_{max})$ of the TOF tip is $NA \approx 1.08$.

Simplifying the whole volume of the diamond as a thin sheet point sources ensemble near the TOF tip will lift up the calculated value from its real value. However, the large refractive index difference between the diamond and its surrounding medium will cause multiple internal reflections at the diamond crystal surface. These reflections will guide part of fluorescence emitted in directions out of the acceptance cone of the TOF back into its acceptance cone near the TOF tip surface. In addition, the wavelength difference between 850nm (at which the fiber parameters are given) and the strongest fluorescence of NV centers (630-780 nm) also will introduce a small deviation between the real fluorescence collection efficiency and the calculated value. However, these simple calculations still illustrate that the TOF tip will enhance the fluorescence collection efficiency significantly.

Since the graded-index core of the GIF625 fiber can partly concentrate the laser light in the central core of the fiber, the non-TOF tip already has a relatively high excitation efficiency in illuminating a micrometer-size diamond attached at the center of its apex. The TOF can further concentrate laser light into the diamond attached on its tip to enhance the fluorescence excitation efficiency. However, the enhancing value will be relatively smaller than the collection efficiency enhancement.

3. Results and discussion

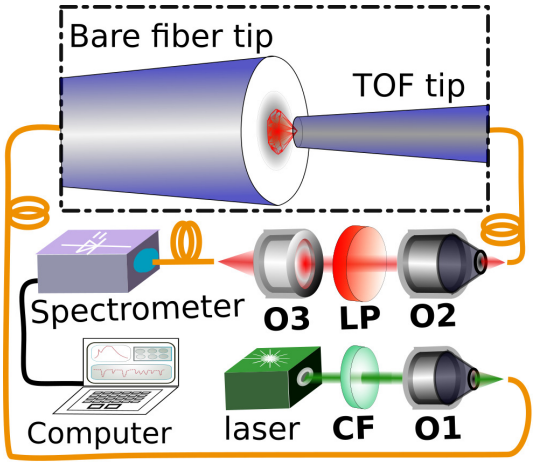

Fig. 4. The assessing setup of TOF tip's fluorescence collection and excitation efficiency. O1, O2, and O3 are objectives; CF is a 512-nm clear-up filter and LP is a 615-nm long-pass filter. The diamond is attached (by UV-curing glue) to the center of a bare fiber tip (enlarged in the dashed box). In the TOF tip or non-TOF tip's fluorescence collection efficiency measuring, the diamond is illuminated under constant laser intensity through the bare fiber tip; the fluorescence is collected by the tested TOF tip or non-TOF tip. In the TOF tip or non-TOF tip's fluorescence excitation efficiency measuring (fiber tip allying need to be reversed in the enlarged dashed box), the fluorescence is collected by the bare fiber tip and the diamond is illuminated through the non-TOF tip or the tested TOF tip with constant laser intensity coupled into them.

The schematic of experimental setup to assess the TOF fluorescence collection and excitation efficiency (Fig. 4), and corresponding microscope images are shown in Fig. 5. The experiment results are shown in Table 1. The "collect" is the intensity ratio of the fluorescence collected from the tested TOF tip and from the comparison non-TOF tip, while the diamond is attached on a bare fiber tip and irradiated with constant laser intensity through the bare fiber tip (Fig. 4). In

Optics EXPRESS

this way, the diamond emits constant fluorescence out, and the intensity of collected fluorescence intensity will only depend on these collection tips' collection ability. Similarly, the "excite" is the intensity ratio of the collected fluorescence from the diamond irradiated under the tested TOF tip and under the comparison non-TOF tip respectively. The fluorescence was collected through the bare fiber tip to which the diamond was attached and, the laser intensity coupled into the TOF tip and the non-TOF tip is constant (the fiber tip alignment needs to be reversed in the enlarged dashed box of Fig. 4). In this way, the bare fiber tip's fluorescence collection efficiency is fixed and, the laser intensities coupled into the TOF tip and non-TOF tip are constant; the collected fluorescence intensity will only depend on these tested tips' excitation ability (concentrate the laser light into the diamond efficiency). In all experiments, both the tested TOF tips and non-TOF tip are dipped with a tiny amount of immersion oil (Fluka 51786, refractive index: 1.512 - 1.522) to enhance its contact to the diamond. The lengths of long TOF and short TOF are ~15 mm and ~1.1 mm respectively (Table 1).

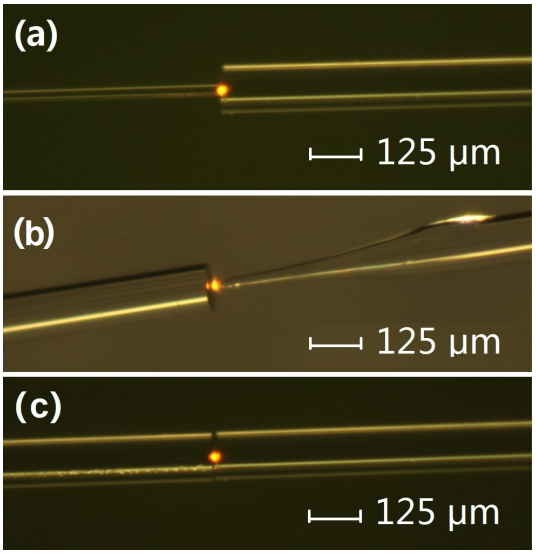

Fig. 5. Microscope images of fluorescence excitation and collection efficiency measuring sets of (a) a long TOF tip, (b) a short TOF tip and (c) a non-TOF tip.

Table 1. Excitation and collection enhancement

diamond size		5 μm		11.7 μm		50 μm	
	tip size	collect[a]	excite[b]	collect[a]	excite[b]	collect[a]	excite[b]
long TOF 1	7.4 μm	15.03	7.68	6.1	2.04	1.35	0.97
long TOF 2	9.6 μm	13.13	7.84	10.79	2.13	1.85	1.11
long TOF 3	17.6 μm	5.35	5.73	8.51	1.93	2.11	1.12
short TOF	12.6 μm	–	–	5.64	2.42	–	–
non-TOF tip	125 μm	1	1	1	1	1	1

[a] ratio of the collected fluorescence intensity of the TOF tip and the non-TOF tip;
[b] ratio of the excited fluorescence intensity of the TOF tip and the non-TOF tip.

Optics EXPRESS

Table 1 indicates that the long TOF tip can obtain a maximum value of 15.03 times the fluorescence collection efficiency of a non-TOF tip, it agrees with our calculated ~16 times based on geometric ray optics. As the TOF and diamond have a dimension scale larger than ten times the wavelengths of the fluorescence and fits the geometric ray optics approximation condition, the calculated value agrees with the experiment results is reasonable. Table 1 also shows that the fluorescence collection efficiency is sensitive to the relative size of the TOF tip and diamond. Generally, a smaller tip size TOF will have a better collection efficiency for a smaller diamond. When the diamond size is set, a TOF tip with a tip size close to the diamond can collect more fluorescence. For NV excitation, if the TOF tip size is too small, it will reduce the excitation efficiency. A TOF tip with a tip size of ~10 μm can get the maximum excitation efficiency. Table 1 also show that a short TOF fluorescence has a lower collection efficiency. This is because the short TOF has a large fiber diameter shrinking rate along the TOF, which cannot meet the adiabatic criteria; as a result, it has a lower fluorescence collection efficiency than that of the long TOF. However, a shorter TOF tip can provide a better mechanical stability than a longer TOF, which may benefit certain applications that require high TOF tip robustness.

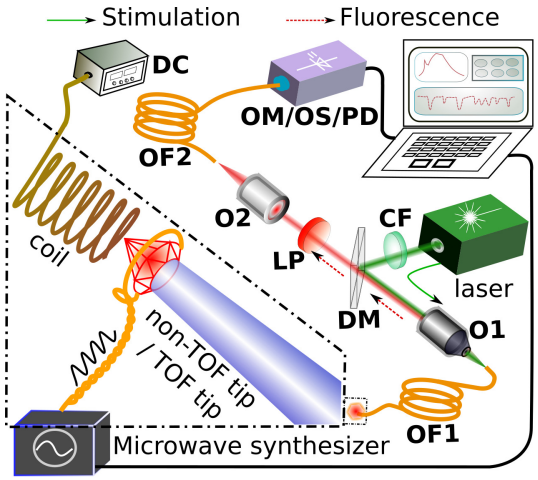

Fig. 6. Fiber-based NV center setup. The green excitation laser (solid arrow), after passing the 532-nm clean-up filter CF and the dichroic mirror DM, is coupled by the objective O1 into the optical fiber OF1 tip where the diamond is attached (dashed triangular box). The fluorescence collected by the non-TOF/TOF tip filtered by 615-nm long-pass filter LP (dashed arrow) and coupled by objective O2 into optical fiber OF2 which is connected to the optical power meter/optical spectrometer/photodiode OM/OS/PD. The DC power supply is used to apply a static magnetic field to the diamond.

Using the setup shown in Fig. 6, we also compared the necessary laser power coupled into several different fiber tips (namely TOFs and non-TOF tip) to collect certain fluorescence power, for example ~262 nW, from diamond attached to it. The comparison of TOF tip and non-TOF tip for same size diamond was carried out by first measuring the fluorescence on the prepared TOF tip and then, cutting off the TOF tip and transferring the same diamond onto the center of the non-TOF tip. The results are shown in Table 2. Figure 7 shows the collected fluorescence spectra of a ~12.5-μm NV enriched diamond attached on a long TOF tip (Fig. 7 (a)), non-TOF tip (Fig. 7 (b)), and a ~156-μm NV enriched diamond attached to a non-TOF tip (with UV-curing glue, Fig. 7 (c)) when coupling ~151 μW of the 532-nm laser into these optical fiber tips. Both Table 2 and Fig. 7 show that TOF can greatly enhance the NV excitation and fluorescence collection efficiency. In Table 1, as the diamonds have already been fixed on the non-TOF tip by UV-curing glue, the measured fluorescence is coupled to the TOF and non-TOF tip from the same surface of

Optics EXPRESS

Table 2. Require excitation laser power to obtain 262 nW of fluorescence

diamond size	fiber end type	tip size	taper length	require laser power [a]
12.5 μm	long taper	12.8 μm	15mm	151 μW
12.5 μm	non-TOF tip	125 μm	–	4.57mW
11.7 μm	short taper	16.8 μm	1 mm	846 μW
11.7 μm	non-TOF tip	125 μm	–	8.07 mW
156 μm	non-TOF tip	125 μm	–	1.52mW
7.9 μm	long taper	12.2 μm	12mm	333 μW
11.3 μm	long taper	13.3 μm	10mm	202 μW

[a] The laser power coupled into the optical fiber attached to the diamond

the diamond crystal (The enlarged box in Fig. 4). In Table 2, the fluorescence coupled to the TOF and the non-TOF tip for the ~12.5-μm and the ~11.7-μm diamonds could be from a different face of the diamond crystal which will result in deviations between the measured results and the real value. Table 2 also shows that a short-TOF exhibits a lower NV excitation and fluorescence collection efficiency than that of the long-TOF.

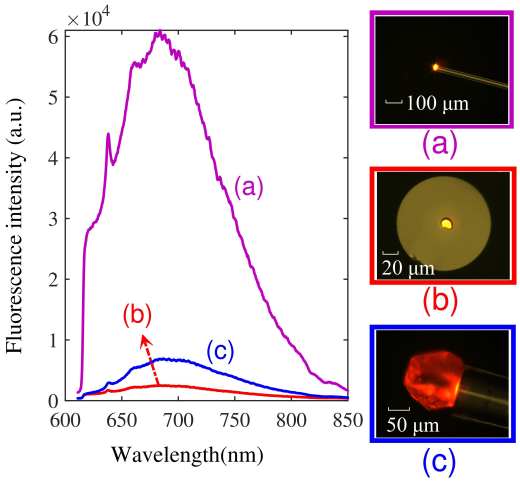

Fig. 7. Comparison of measured fluorescence spectra. In all cases, the excitation laser power launched into the fiber is ~151 μW. (a) is the spectrum of a ~12.5-μm diamond on a TOF tip, (b) is the spectrum of a ~12.5-μm diamond on the center of a cleaved flat fiber end, and (c) is the spectrum of a ~156-μm diamond on a non-TOF tip. The inset shows microscope images of these samples. The length of the TOF is ~15 mm, and its tip diameter is ~12.8 μm. The fiber diameter is ~125 μm.

Some specially designed photonic microstructure optical fibers also deliver a high NA which will benefit the endoscope-type NV sensor building [24]. We used the setup shown in Fig. 6 and investigated the possibility of using an ultra-high NA photonic microstructure fiber MM-HNA-35 (NKT Photonics, Denmark. Core diameter:35 μm) in fluorescence excitation and collection from sub-ten micrometers diamonds. We find that the MM-HNA-35 fiber is poor at excitation NV centers in diamonds smaller than 10 μm as its core cannot focus the laser light into its center (Fig.

Optics EXPRESS

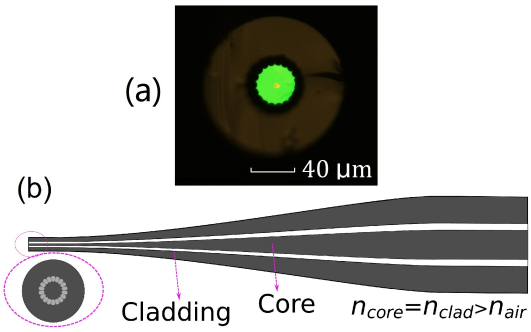

Fig. 8. (a) Microscope images of a ~5.2-μm diamond on the center of the cleaved non-TOF tip of the Ultra-high NA photonic microstructure fiber. (b) Schematic diagram of the tapered ultra-high NA photonic microstructure fiber.

8(a)). In a MM-HNA-35 fiber based TOF, most of the fluorescence entered the cladding region (accounts up to $1-(35/125)^2 \approx 92\%$ of the TOF tip), and cannot be coupled into the core of the fiber. This is because the air isolation band between the core and cladding will partly remain in the TOF (Fig. 8(b) shows its schematic illustration). Thus, it is critical to match the sizes of the diamond and the high NA photonic microstructure fiber core or TOF core to obtain high NV excitation and fluorescence collection efficiency, in such kind of high NA fiber configurations as endoscope-type NV sensors.

In addition, this TOF tip can combine the micro-concave technique [35] to further enhance the fluorescence excitation and collection efficiency. As the micro-concave mirror can focus back the fluorescence emitted in the opposite direction of the TOF in a smaller incidence angle, and the TOF has a relatively large fluorescence acceptance angle, this combination can greatly improve the system's fluorescence collection. Ideally, if the matched micro-concave mirror is in parabolic reflector shape, the total fluorescence collection efficiency will be over 50% + TOF tip (without the micro-concave mirror) fluorescence collection efficiency. If the TOF tip's fluorescence collection efficiency is 5%, combining it with a matched micro parabolic mirror will reach a fluorescence collection efficiency of over 55%, and enhance over 10 times the fluorescence collection efficiency. In a simple experiment evaluation for an unmatched relatively big micro-concave mirror, we obtained only ~ 2.2 times the collected fluorescence efficiency of the TOF tip without using the micro-concave mirror.

The excitation efficiency of NV-center on a TOF tip is the number of generated fluorescence photons divided by the number of 532-nm photons coupled into the optical fiber. Taking the ~12.5-μm diamond on the ~12.8-μm TOF tip for example. The excitation laser is ~151 μW and the collected fluorescence is ~262 nW. Using a wavelength calibrated calculation, we obtained a collected fluorescence photon number and incidence laser photon number ratio $\sigma \approx 1.864/1000$. Divided by the calculated fluorescence collection efficiency 5.3%, an NV-center excitation efficiency of 3.5% is obtained.

Since the NVs' excitation and fluorescence collection enhancement greatly benefits the NV-spin magnetometry applications [1,2], utilizing a TOF tip will certainly improve its sensitivity. To give a hint on this improvement, we resorted to CW-ODMR by detecting the fluorescence emission and varying the frequency of microwaves that induce spin transitions. We performed a series of experiments and compared the ODMR magnetic field detection sensitivity of two diamonds crystals bonded on TOF tip and non-TOF tip. The results (Fig. 9) shown that under the same excitation laser power, the small ~7.9-μm diamond on the 12.5-μm TOF tip (Fig. 9(a)) have about 28.3 times the sensitivity of the ~11.4-μm diamond on the non-TOF tip. This value is much higher than the $\sqrt{n}$ ($\sqrt{n} \approx 5$) times of the fluorescence intensity. We believe this is because our

Optics EXPRESS

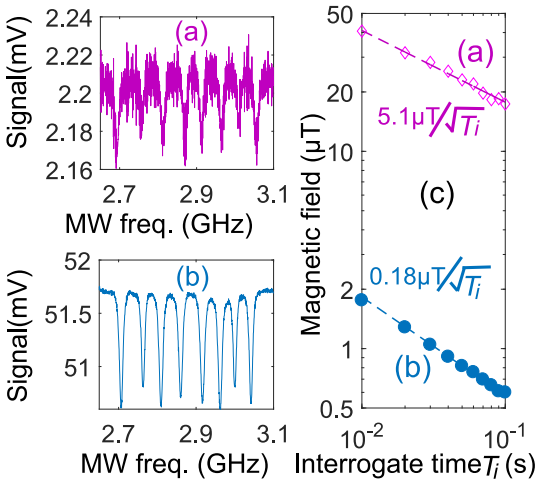

Fig. 9. (a) the ODMR spectra of a ~11.4-μm diamond UV-curing glue bonded on a non-TOF tip center in a 9.6 mT magnetic field. (b) the ODMR spectra of the UV-curing glue bonded~7.9-μm diamond on TOF tip in a 9.0 mT magnetic field. The laser power used for both cases was same, ~36.5 μW. The signals are read by a photodiode detector. (c) The Magnetic field sensitivity comparison of the two sensor heads (a) and (b).

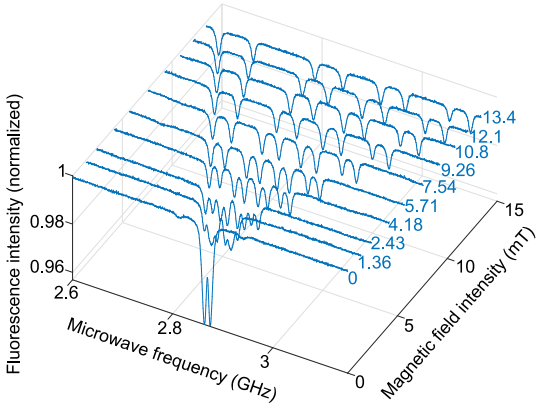

Fig. 10. ODMR spectra of the NV-center ensembles in a ~11.3-μm diamond bonded on the tip of a ~10-mm long TOF recorded for various magnetic field values (Fluorescence intensity have been normalized). The TOF tip' diameter is ~13.3 μm. The magnetic field was applied by the DC coil. The test was executed using the Fig.6 setup, the laser power used to excite the diamond was 0.239 mW and the collected fluorescence was 0.309 μW (the power meter was set at 635 nm).

measurement is far from the photon shot-noise limit. In the non-TOF tip case, the fluorescence intensity is too low; hence the system noise limits the measured magnetic sensitivity. As a demonstration, we bonded a ~11.3-μm diamond on TOF tip by UV-curing glue and used it for measuring a DC magnetic field (Fig. 10). We used only 0.238 mW of laser power to initialize the NV-center ensemble, and -15 dBm of microwave power to induce the electronic spin resonance between the ms=0 spin state and the ms=±1 states of the NV centers. DC current was applied to a coil to vary the external magnetic field. Figure 10 shows the single-run ODMR spectra at various magnetic fields; the signals are obtained without utilizing any special techniques such as lock-in amplification or data averaging.

Optics EXPRESS

4. Conclusion

To summarize, we have fabricated a quasi-adiabatic TOF tip that performs similarly to an objective in a classical optical path for both the excitation and collection of the fluorescence from NV centers in micrometer-sized diamond. Calculation shows that the TOF tip possesses an ultra-high NA; experiments demonstrate that this technique can greatly enhance the excitation and fluorescence collection efficiency. We used this enhancing to boost the magnetic sensitivity of micro-sized NV endoscope-type magnetometer and achieve a sensitivity of 180 nT$\sqrt{Hz}$ for a ~7.9-μm diamond crystal for DC magnetic field sensing. Furthermore, this improved excitation and collection enhancements reduce the size of the diamond sample that is required for precision sensing, potentially increasing the spatial resolution (less than 8 μm) and retains the flexibility of optical fiber-based NV endoscope-type sensors.

Funding

Max-Planck Society, Niedersächsisches Ministerium für Wissenschaft und Kultur, DFG Research Center Nanoscale Microscopy and Molecular Physiology of the Brain.

Acknowledgments

The authors thank Dr. Andrii Lazariev for critical reading of the manuscript.

References

1. J. M. Taylor, P. Cappellaro, L. Childress, L. Jiang, D. Budker, P. R. Hemmer, A. Yacoby, R. Walsworth, and M. D. Lukin, "High-sensitivity diamond magnetometer with nanoscale resolution," Nat Phys **4**, 810–816 (2008).
2. L. M. Pham, D. L. Sage, P. L. Stanwix, T. K. Yeung, D. Glenn, A. Trifonov, P. Cappellaro, P. R. Hemmer, M. D. Lukin, H. Park, A. Yacoby, and R. L. Walsworth, "Magnetic field imaging with nitrogen-vacancy ensembles," New J. Phys. **13**, 045021 (2011).
3. L. Rondin, J.-P. Tetienne, T. Hingant, J.-F. Roch, P. Maletinsky, and V. Jacques, "Magnetometry with nitrogen-vacancy defects in diamond," Reports on Prog. Phys. **77**, 056503 (2014).
4. F. Dolde, M. W. Doherty, J. Michl, I. Jakobi, B. Naydenov, S. Pezzagna, J. Meijer, P. Neumann, F. Jelezko, N. B. Manson, and J. Wrachtrup, "Nanoscale detection of a single fundamental charge in ambient conditions using the NV^- center in diamond," Phys. Rev. Lett. **112**, 097603 (2014).
5. P. Neumann, I. Jakobi, F. Dolde, C. Burk, R. Reuter, G. Waldherr, J. Honert, T. Wolf, A. Brunner, J. H. Shim, D. Suter, H. Sumiya, J. Isoya, and J. Wrachtrup, "High-precision nanoscale temperature sensing using single defects in diamond," Nano Lett. **13**, 2738–2742 (2013). PMID: 23721106.
6. G. Kucsko, P. C. Maurer, N. Y. Yao, M. Kubo, H. J. Noh, P. K. Lo, H. Park, and M. D. Lukin, "Nanometre-scale thermometry in a living cell," Nature **500**, 54–58 (2013).
7. D. M. Toyli, C. F. de las Casas, D. J. Christle, V. V. Dobrovitski, and D. D. Awschalom, "Fluorescence thermometry enhanced by the quantum coherence of single spins in diamond," PNAS **110**, 8417–8421 (2013).
8. J. R. Rabeau, S. T. Huntington, A. D. Greentree, and S. Prawer, "Diamond chemical-vapor deposition on optical fibers for fluorescence waveguiding," Appl. Phys. Lett. **86**, 134104 (2005).
9. M. R. Henderson, B. C. Gibson, H. Ebendorff-Heidepriem, K. Kuan, S. Afshar V., J. O. Orwa, I. Aharonovich, S. Tomljenovic-Hanic, A. D. Greentree, S. Prawer, and T. M. Monro, "Hybrid materials: Diamond in tellurite glass: a new medium for quantum information (adv. mater. 25/2011)," Adv. Mater. **23**, 2772–2772 (2011).
10. Y. Ruan, H. Ji, B. C. Johnson, T. Ohshima, A. D. Greentree, B. C. Gibson, T. M. Monro, and H. Ebendorff-Heidepriem, "Nanodiamond in tellurite glass part ii: practical nanodiamond-doped fibers," Opt. Mater. Express **5**, 73–87 (2015).
11. T. Schröder, A. W. Schell, G. Kewes, T. Aichele, and O. Benson, "Fiber-integrated diamond-based single photon source," Nano Lett. **11**, 198–202 (2011).
12. L. Mayer and T. Debuisschert, "Direct optical interfacing of cvd diamond for deported sensing experiments involving nitrogen-vacancy centres," physica status solidi (a) **213**, 2608–2613 (2016).
13. M. Gregor, R. Henze, T. SchrÃűder, and O. Benson, "On-demand positioning of a preselected quantum emitter on a fiber-coupled toroidal microresonator," Appl. Phys. Lett. **95**, 153110 (2009).
14. T. Schröder, M. Fujiwara, T. Noda, H.-Q. Zhao, O. Benson, and S. Takeuchi, "A nanodiamond-tapered fiber system with high single-mode coupling efficiency," Opt. Express **20**, 10490–10497 (2012).
15. R. Albrecht, A. Bommer, C. Pauly, F. MÃijcklich, A. W. Schell, P. Engel, T. SchrÃűder, O. Benson, J. Reichel, and C. Becher, "Narrow-band single photon emission at room temperature based on a single nitrogen-vacancy center coupled to an all-fiber-cavity," Appl. Phys. Lett. **105**, 073113 (2014).
16. L. Liebermeister, F. Petersen, A. v. MÃijnchow, D. Burchardt, J. Hermelbracht, T. Tashima, A. W. Schell, O. Benson, T. Meinhardt, A. Krueger, A. Stiebeiner, A. Rauschenbeutel, H. Weinfurter, and M. Weber, "Tapered fiber coupling

Optics EXPRESS

of single photons emitted by a deterministically positioned single nitrogen vacancy center," Appl. Phys. Lett. **104**, 031101 (2014).
17. M. Fujiwara, H.-Q. Zhao, T. Noda, K. Ikeda, H. Sumiya, and S. Takeuchi, "Ultrathin fiber-taper coupling with nitrogen vacancy centers in nanodiamonds at cryogenic temperatures," Opt. Lett. **40**, 5702–5705 (2015).
18. R. N. Patel, T. Schröder, N. Wan, L. Li, S. L. Mouradian, E. H. Chen, and D. R. Englund, "Efficient photon coupling from a diamond nitrogen vacancy center by integration with silica fiber," Light. Sci. Appl. **5**, e16032 (2016).
19. V. V. Vorobyov, V. V. Soshenko, S. V. Bolshedvorskii, J. Javadzade, N. Lebedev, A. N. Smolyaninov, V. N. Sorokin, and A. V. Akimov, "Coupling of single nv center to adiabatically tapered opticalsingle mode fiber," The Eur. Phys. J. D **70**, 269 (2016).
20. M. J. Burek, C. Meuwly, R. E. Evans, M. K. Bhaskar, A. Sipahigil, S. Meesala, B. Machielse, D. D. Sukachev, C. T. Nguyen, J. L. Pacheco, E. Bielejec, M. D. Lukin, and M. Lončar, "Fiber-coupled diamond quantum nanophotonic interface," Phys. Rev. Appl. **8**, 024026 (2017).
21. I. V. Fedotov, L. V. Doronina-Amitonova, A. A. Voronin, A. O. Levchenko, S. A. Zibrov, D. A. Sidorov-Biryukov, A. B. Fedotov, V. L. Velichansky, and A. M. Zheltikov, "Electron spin manipulation and readout through an optical fiber," Sci. Reports **4**, 5362 (2014).
22. I. V. Fedotov, L. V. Doronina-Amitonova, D. A. Sidorov-Biryukov, N. A. Safronov, S. Blakley, A. O. Levchenko, S. A. Zibrov, A. B. Fedotov, S. Y. Kilin, M. O. Scully, V. L. Velichansky, and A. M. Zheltikov, "Fiber-optic magnetic-field imaging," Opt. Lett. **39**, 6954–6957 (2014).
23. I. V. Fedotov, S. Blakley, E. E. Serebryannikov, N. A. Safronov, V. L. Velichansky, M. O. Scully, and A. M. Zheltikov, "Fiber-based thermometry using optically detected magnetic resonance," Appl. Phys. Lett. **105**, 261109 (2014).
24. I. V. Fedotov, S. M. Blakley, E. E. Serebryannikov, P. Hemmer, M. O. Scully, and A. M. Zheltikov, "High-resolution magnetic field imaging with a nitrogen-vacancy diamond sensor integrated with a photonic-crystal fiber," Opt. Lett. **41**, 472–475 (2016).
25. M. M. Dong, Z. Z. Hu, Y. Liu, B. Yang, Y. J. Wang, and G. X. Du, "A fiber based diamond rf b-field sensor and characterization of a small helical antenna," Appl. Phys. Lett. **113**, 131105 (2018).
26. J. D. Love, W. M. Henry, W. J. Stewart, R. J. Black, S. Lacroix, and F. Gonthier, "Tapered single-mode fibers and devices: Part 1, adiabaticity criteria," IEE Proc., Optoelectron. **138**, 343–354 (1991).
27. R. J. Black, S. Lacroix, F. Gonthier, and J. D. Love, "Tapered single mode fibers and devices: Part 2, experimental and theoretical quantification." IEE Proc. **138**, 355–364 (1991).
28. optgeo, "optgeo," http://jeanmarie.biansan.free.fr/optgeo.html.
29. T. A. Birks and Y. W. Li, "The shape of fiber tapers," J. Light. Technol. **10**, 432–438 (1992).
30. A. Stiebeiner, R. Garcia-Fernandez, and A. Rauschenbeutel, "Design and optimization of broadband tapered optical fibers with a nanofiber waist," Opt. Express **18**, 22677–22685 (2010).
31. S. Pricking and H. Giessen, "Tapering fibers with complex shape," Opt. Express **18**, 3426–3437 (2010).
32. H. Latifi, M. I. Zibaii, S. M. Hosseini, and P. Jorge, "Nonadiabatic tapered optical fiber for biosensor applications," Photonic Sensors **2**, 340–356 (2012).
33. S. Harun, K. Lim, C. Tio, K. Dimyati, and H. Ahmad, "Theoretical analysis and fabrication of tapered fiber," Optik **124**, 538–543 (2013).
34. T.-J. Wu, Y.-K. Tzeng, W.-W. Chang, C.-A. Cheng, Y. Kuo, C.-H. Chien, H.-C. Chang, and J. Yu, "Tracking the engraftment and regenerative capabilities of transplanted lung stem cells using fluorescent nanodiamonds," Nat. Nano. **8**, 682–689 (2013).
35. D. Duan, V. K. Kavatamane, S. R. Arumugam, G. Rahane, Y.-K. Tzeng, H.-C. Chang, H. Sumiya, S. Onoda, J. Isoya, and G. Balasubramanian, "Enhancing fluorescence excitation and collection from the nitrogen-vacancy center in diamond through a micro-concave mirror," Appl. Phys. Lett. **113**, 041107 (2018).